Origin of Stereoselectivities in Asymmetric Alkoxyselenenylations

4 AUTHORS, INCLUDING:

Martin Spichty
Ecole normale supérieure de Lyon

31 PUBLICATIONS   **682** CITATIONS

Origin of Stereoselectivities in Asymmetric Alkoxyselenenylations

Xue Wang,† K. N. Houk,*,† Martin Spichty,‡ and Thomas Wirth‡

*Contribution from the Department of Chemistry and Biochemistry, University of California,
Los Angeles, California 90095, and Institut für Organische Chemie der Universität Basel,
St. Johanns-Ring 19, CH-4056 Basel, Switzerland*

Received February 16, 1999

Abstract: Asymmetric alkoxyselenenylations of alkenes have been studied by B3LYP/3-21G, B3LYP/6-31G*, and SCI-PCM calculations. Stereoselectivities can be rationalized by the relative stabilities of transition states for attack of nucleophiles on seleniranium intermediates. A model to explain and predict stereoselectivities has been developed.

Introduction

The reactions of areneselenenyl halides with alkenes exhibit high Markownikoff regioselectivity and anti stereoselectivity.[1] The mechanisms have been studied since the 1970s.[2] The two steps involve the formation of areneseleniranium intermediates **1**, followed by nucleophilic attack of a halide or alcohol to give products **2**, either β-haloalkyl selenides or β-alkoxyl selenides (Scheme 1). The reaction occurs in a stereospecific anti manner, with the nucleophile attacking the more substituted carbon unless the carbon is substituted with very bulky *tert*-butyl or cyclohexyl groups.[3] The rate-determining step depends on the substituents on both areneselenium and alkene compounds, as well as temperature and solvent.[4] Most frequently, the first step is reversible so that the second step determines the stereochemistry of products. At low temperatures, this reaction is under kinetic control.[5−7]

Chiral aryl diselenides have been extensively studied by various research groups—Back, Déziel, Fukuzawa, Tomoda, Uemura, and Wirth. This work has been reviewed extensively.[8] Déziel and co-workers reported a C_2 symmetric diselenide **3** in 1993,[9] while Wirth and co-workers described the more acces-
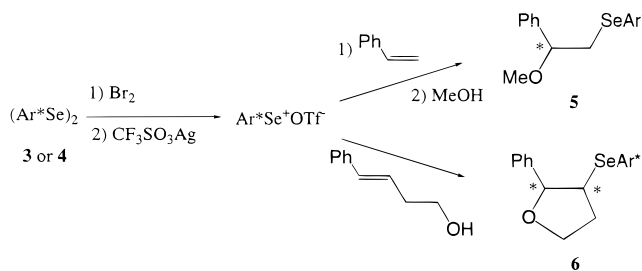
Scheme 1. Haloselenenylation and Alkoxyselenenylation Reactions X = Cl or Br; Y = Cl, Br, or OR
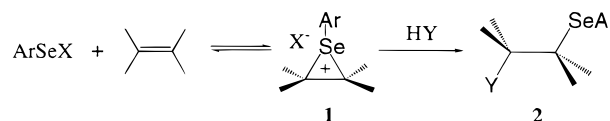
Scheme 2. The Chiral Diselenide Reagents of Déziel (**3**) and Wirth (**4**)
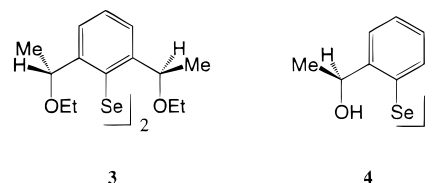
Scheme 3. The Methoxyselenenylation of Styrene and the Selenocyclization of (*E*)-4-phenyl-3-butenol Leading to Compounds 5 and 6 (Ar* Is the Chiral Group)

sible diselenide **4** in 1995 (Scheme 2).[10] The diselenides **3** and **4** are transformed into the corresponding areneselenenyl triflates, and these highly electrophilic reagents have been used in stereoselective alkoxyselenenylations of alkenes or in seleno-cyclizations to yield **5** (with **3**, 91% de, 89% yield; with **4**, 83% de, 67% yield) and **6** (with **3**, 85% de, 92% yield; with **4**, 84% de, 87% yield) in good yields and stereoselectivities as shown in Scheme 3. Tomoda and co-workers designed and tested binaphthyl and chiral tertiary amino-substituted selenium re-

† University of California.
‡ Institut für Organische Chemie der Universität Basel.

(1) Lautenschlaeger, F. *J. Org. Chem.* **1969,** *34,* 4002−4006. Garratt, D. G.; Schmid, G. H. *Can. J. Chem.* **1974,** *52,* 3599−3606. Sharpless, K. B.; Lauer, R. F. *J. Org. Chem.* **1974,** *39,* 429−430. Clive, D. L. J. *J. Chem. Soc., Chem. Commun.* **1974,** 100. Schmid, G. H.; Garratt, D., G. *Tetrahedron* **1978,** *34,* 2869−2872.

(2) Schmid, G. H.; Garratt, D. G. *Tetrahedron Lett.* **1975,** 3991−3994. Rémion, J.; Krief, A. *Tetrahedron Lett.* **1976,** 3743−3746. Garratt, D. G. *Can. J. Chem.* **1979,** *57,* 2180−2184. Garratt, D. G.; Kabo, A. *Can. J. Chem.* **1980,** *58,* 1030−1041.

(3) Patai, S. *The Chemistry of Double-Bonded Functional Groups, Part 2*; John Wiley & Sons: New York, 1989; pp 859−861.

(4) Schmid, G. H.; Garratt, D. G. *J. Org. Chem.* **1983,** *48,* 4169−4172.

(5) Nicolaou, K. C.; Seitz, S. P.; Sipio, W. J.; Blount, J. F. *J. Am. Chem. Soc.* **1979,** *101,* 3884−3893.

(6) Fujita, K−i.; Murata, K.; Iwaoka, M.; Tomoda, S. *Tetrahedron* **1997,** *53,* 2029−2048.

(7) Tomoda, S.; Iwaoka, M. *Chem. Lett.* **1988,** 1895−1898.

(8) See the following review: Wirth, T. *Tetrahedron* **1999,** *55,* 1−28 and references therein.

(9) Déziel, R.; Goulet, S.; Grenier, L.; Bordeleau, J.; Bernier, J. *J. Org. Chem.* **1993,** *58,* 3619−3621. Déziel, R.; Malenfant, E. *J. Org. Chem.* **1995,** *60,* 4660−4662. Déziel, R.; Malenfant, E.; Bélanger, G. *J. Org. Chem.* **1996,** *61,* 1875−1876. Déziel, R.; Malenfant, E.; Thibault, C. *Tetrahedron Lett.* **1998,** *39,* 5493−5496.

(10) Wirth, T. *Angew. Chem.* **1995,** *107,* 1872−1873. Wirth, T. *Angew. Chem., Int. Ed. Engl.* **1995,** *34,* 1726−1728. Wirth, T. *Liebigs Ann./Recueil* **1997,** 2189−2196. Fragale, G.; Wirth, T. *Eur. J. Org. Chem.* **1998,** 1361−1369.
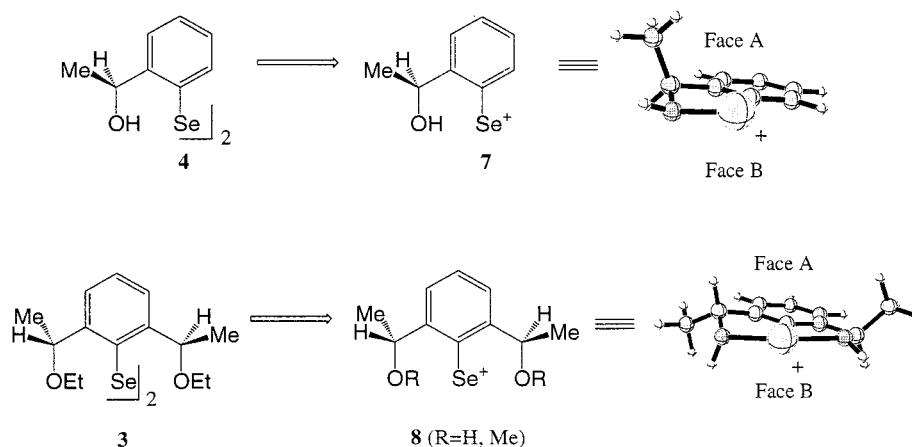
Figure 1. B3LYP/3-21G optimized geometries of cations **7** and **8** from the Wirth and the Déziel reagents.
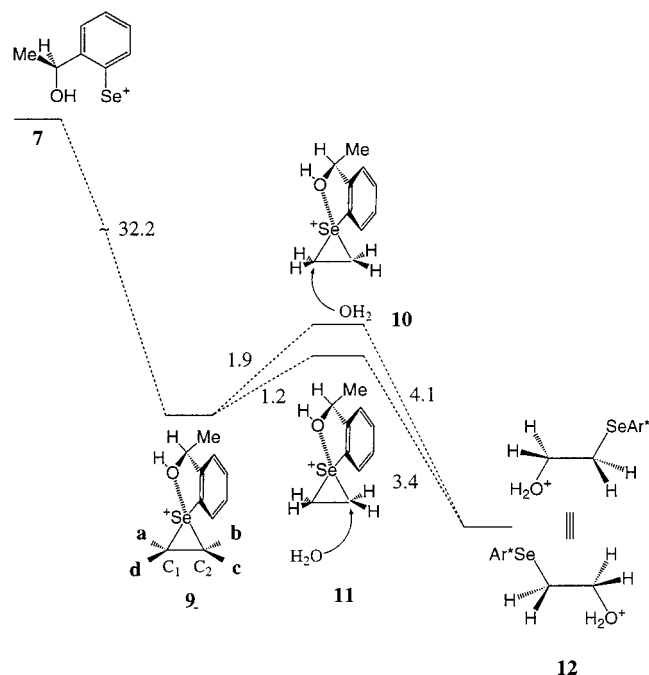
Figure 2. Computed energetics (B3LYP/6-31G*//B3LYP/3-21G) for the reaction of the Wirth reagent and ethylene. All energies are in kcal/mol.
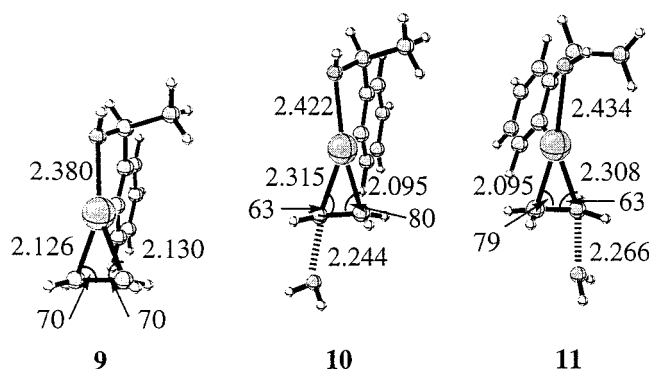
Figure 3. Geometrical parameters of the intermediate **9** and transition states **10** and **11** (distances in Å, angles in deg).

agents.[11] Camphorselenenyl reagents were also reported for asymmetric alkoxyselenenylations.[12] The origin of the stereoselectivities has been explored,[13] and new reagents have been investigated.[7,14]

In this paper, we describe the theoretical explanation of the

Table 1. The Intermediate Formed from the Wirth Reagent and Ethylene with the Relative Energies of the Intermediates Substituted by Methyl or Phenyl

substituent	a	b	c	d
methyl	2.3	1.2	0	0.2
phenyl	1.4	0.6	0.3	0

chiral reagents developed by Déziel and Wirth for asymmetric selenenylations.

Computational Methods

Geometries were fully optimized with the B3LYP density functional method and the 3-21G basis set. Minima and transition states were characterized by vibrational frequency calculations. Energies were also computed at the B3LYP/6-31G* level with SCI-PCM solvation calculations on 3-21G geometries.[15]

(11) Iwaoka, M.; Tomoda, S. *J. Org. Chem.,* **1995**, *60,* 5299–5302. Fujita, K. I.; Murata, K.; Iwaoka, M.; Tomoda, S. *J. Chem. Soc., Chem. Commun.* **1995**, 1641–1642. Fujita, K.; Murata, K.; Iwaoka, M.; Tomoda, S. *Tetrahedron Lett.* **1995**, *36,* 5219–5222. Fujita, K.; Murata, K.; Iwaoka, M.; Tomoda, S. *Heteroatom Chem.* **1995**, *6,* 247–257. Fujita, K.; Iwaoka, M.; Tomoda, S. *Chem. Lett.* **1994**, 923–926. Iwaoka, M.; Tomoda, S. *J. Chem. Soc., Chem. Commun.* **1992**, 1165–1167. Fujita, K.; Iwaoka, M.; Tomoda, S. *Chem. Lett.* **1992**, 1123–1124. Tomoda, S.; Fujita, K.; Iwaoka, M. *Chem. Commun.* **1990**, 129–131. Tomoda, S.; Usuki, Y. *Chem. Lett.* **1989**, 1235–1236.

(12) Back, T. G.; Nan, S. *J. Chem. Soc., Perkin Trans. 1* **1998**, 3123–3124. Tiecco, M.; Testaferri, L.; Santi, C.; Marini, F.; Bagnoli, L.; Temperini, A. *Tetrahedron Lett.* **1998**, *39,* 2809–2812. Back, T. G.; Dyck, B. P. *J. Am. Chem. Soc.* **1997**, *119,* 2079–2083. Back, T. G.; Dyck, B. P. *J. Chem. Soc., Chem. Commun.* **1996**, 2567–2568. Back, T. G.; Dyck, B. P.; Parvez, M. *J. Chem. Soc., Chem. Commun.* **1994**, 515–516.

(13) Wirth, T.; Fragale, G. *Chem.—Eur. J.* **1997**, *3,* 1894–1902.

(14) Fragale, G.; Neuburger, M.; Wirth, T. *Chem. Commun.* **1998**, 1867–1868.

(15) Frisch, M. J.; Trucks, G. W.; Schlegel, H. B.; Gill, P. M. W.; Johnson, B. G.; Robb, M. A.; Cheeseman, J. R.; Keith, T. A.; Petersson, G. A.; Montgomery, J. A.; Raghavahari, K.; Al-Laham, M. A.; Zakrzewski, V. G.; Ortiz, J. V.; Foresman, J. B.; Cioslowski, J.; Stefanov, B. B.; Nanayakkara, A.; Challacombe, M.; Peng, C. Y.; Ayala, P. Y.; Chen, W.; Wong, M. W.; Andres, J. L.; Replogle, E. S.; Gomperts, R.; Martin, R. L.; Fox, D. J.; Binkley, J. S.; Defrees, D. J.; Baker, J.; Stewart, J. P.; Head-Gordon, M.; Gonzales, C.; Pople, J. A. *Gaussian 94,* revision A.1; Gaussian, Inc: Pittsburgh, PA, 1995.
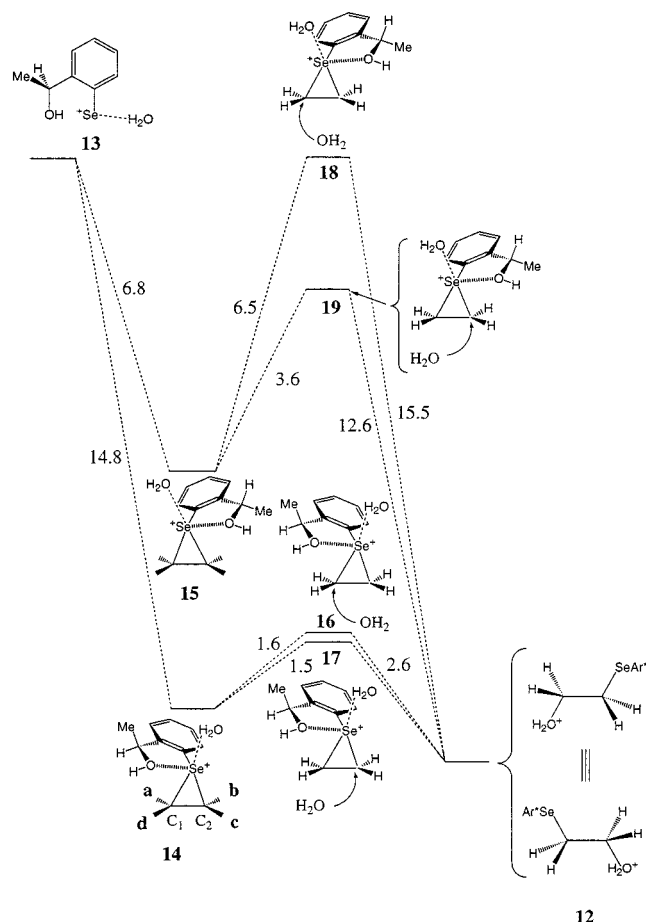
Figure 4. Computed energetics for the reaction of the Wirth reagent with ethylene with one water molecule chelating selenium.

Table 2. The Intermediate Formed from the H_2O-Chelated Wirth Reagent and Ethylene with the Relative Energies of the Intermediates Substituted by Methyl or Phenyl, along with π-Stacking of Intermediate **22a** Shown below
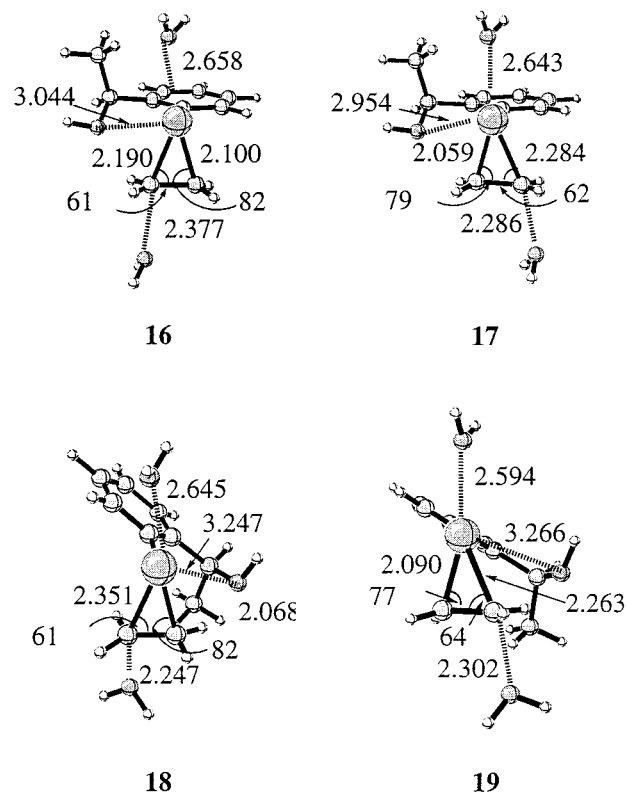

substituent	a	b	c	d
methyl	1.1	1.5	0	0.6
phenyl	0	1.1	0.5	0.5
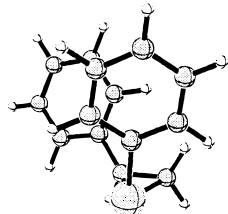
22a

Results and Discussion

1. Geometry of Reactants. The free cations and cations coordinated to model leaving groups have both been studied. Optimized structures of **7**, a model for the selenium cation derived from **4**, and **8**, a model for the selenium cation derived

Figure 5. Geometrical parameters of the transition states **16**, **17**, **18**, and **19** (distances in Å, angles in deg).

from **3**, are shown in Figure 1. The hydroxyl groups form chelates with selenium with bond lengths of 1.93−2.11 Å. This interaction inhibits the rotation of the aryl group around the Se−C bond. The chiral auxiliaries on the aryl group are also fixed, which causes one face of the aryl group to be less hindered than the other. For **7**, there is one methyl group in face **A**, and a proton in face **B**. Cation **8** has C_2 symmetry so that there is no difference between face **A** and face **B**, but the lower right and upper left quadrants are less hindered than the other quadrants.

2. Reaction Pathways. a. Model of the Wirth Reagent. There are two steps involved in the reaction. The first step, the addition of a free selenium cation **7** to an alkene, is very exothermic (Figure 2). No transition state could be located. This is a result of our omission of the leaving group (triflate on the selenium reagent) and solvent, both of which would stabilize the reactant relative to the seleniranium intermediates. Intermediate **9** has no symmetry. The distances from the aryl group on selenium to the four protons, **a−d**, of the alkene are different (Figure 2). Positions **a** and **b** are neighboring the aryl group, and positions **c** and **d** are away from the aryl group.

The relative stabilities of intermediates with methyl or phenyl substituted at positions **a−d** were calculated. Results are summarized in Table 1. With both methyl and phenyl groups, positions **c** and **d** away from the aromatic substituent of selenide are more stable than **a** and **b**, for steric reasons.

The geometries of the corresponding intermediates from reactions of styrene were optimized earlier at the MP2/3-21G* level.[16] The geometries are quite different so that the relative energies of isomeric intermediates are different from B3LYP/ 3-21G results. The geometries by MP2 are, however, similar to those of the coordinated species, **13**, described below.

(16) Wirth, T.; Fragale, G.; Spichty, M. *J. Am. Chem. Soc.* **1998**, *120*, 3376−3381.
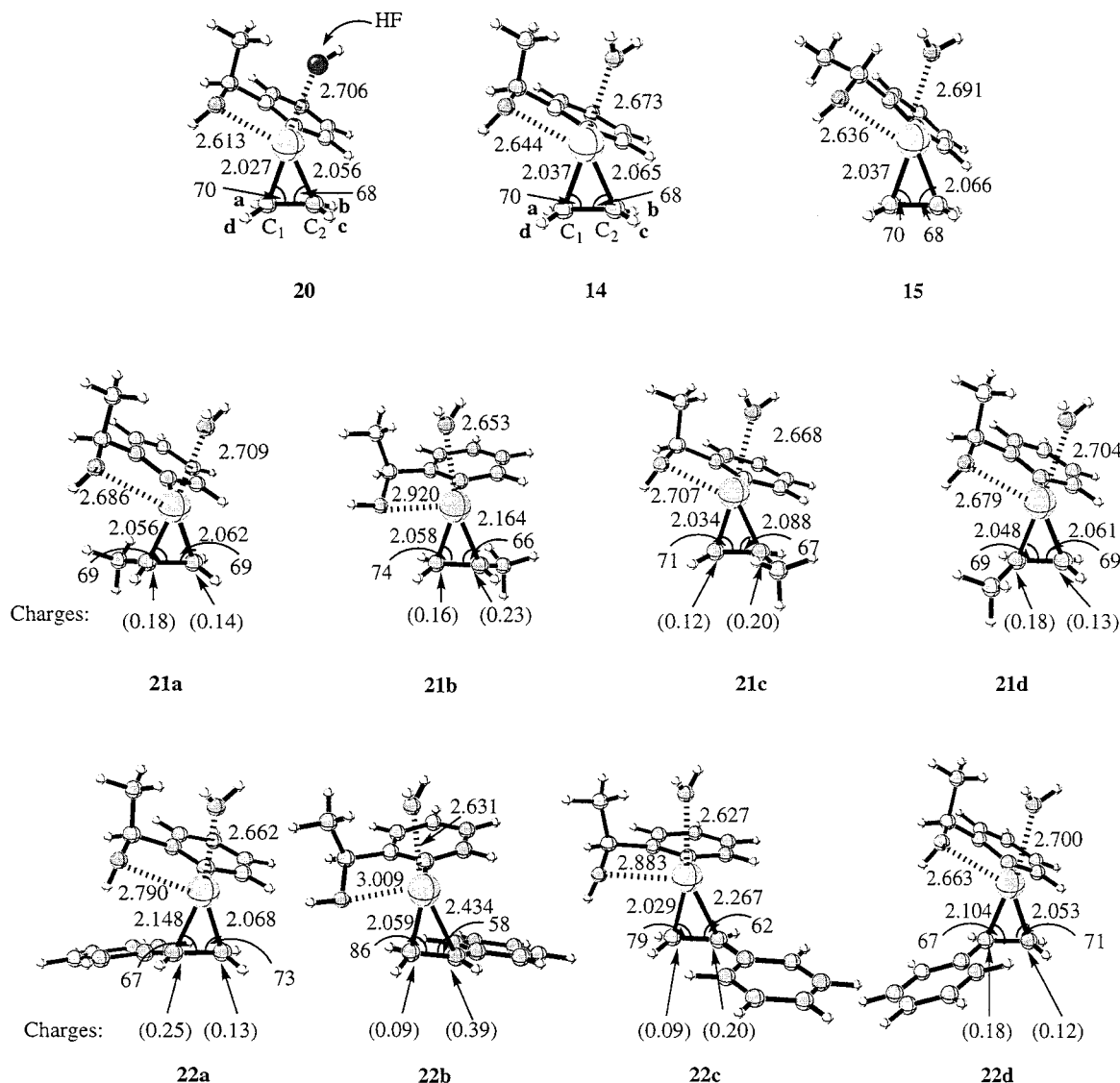
Figure 6. Geometrical parameters of the intermediates (distances in Å, angles in deg, numbers in parentheses are the sum of Mulliken charges of the carbon plus attached hydrogen and substituents).

In the second step of the reaction, an alcohol, simulated in all calculations by water, attacks **9**. The nucleophile approaches in an S_N2 fashion, from the backside of **9**. A water molecule may attack at C_1 or C_2 to give transition states **10** and **11**. In the absence of substituents at the double bond, transition state **11** is slightly favored (Figure 3).

The free aryl selenium cation is probably not formed in the reactions, and so a water molecule was added, coordinated to Se^+, as a model for a leaving group or solvent association. The use of a neutral leaving group allows gas-phase calculations to be performed, where an anion leaving group or counterion would be reluctant to dissociate in the gas phase. Calculations have been done on reactions of structure **13** with one water added, a model for the Wirth reagent (Figure 4). The reactions are performed in mixed solvents of diethyl ether and methanol, and methanol is very likely to chelate to the cationic species. Model **13** is likely to better mimic these reactions in solution. The MeOH−Se coordination is relatively weak and reversible.[3]

Figure 4 shows that the alkene and **13** now interact in a more face to face fashion, because of the water chelation, which alters the aryl group conformation. The alkene can coordinate on either face of **13**. Face **B** of **13** is less crowded and more easily

coordinated. Intermediate **14** is much more stable than **15**. The four positions **a**−**d** of seleniranium intermediate **14** are differentiated more than the four positions of the intermediate **9**. Table 2 gives the relative energies of methyl- and phenyl-substituted versions of **14**. Positions **a** and **b** are closer to the aryl surface, and a phenyl substituent can π-stack in position **a**, as shown in Table 2, **22a**. Steric hindrance is most severe in **b**. Phenyl prefers position **a**. Methyl substituents still favor positions **c** or **d** to minimize steric hindrance.

The structure of the intermediate and the rate of attack of alcohol on the seleniranium intermediate determine the regio- and stereochemistry of the products. The four possible transition states formed by attack of water on C_1 or C_2 of **14** or **15** are shown in Figure 5. The nucleophile attacks C_1 or C_2 from the backside of **14** in an S_N2 fashion. The C−water distance in the transition state **16** is 2.377 Å, while this distance in **17** is 2.286 Å. The transition state **17** is somewhat later than **16**, and the activation barrier for nucleophile to attack C_2 is about 0.1 kcal/mol lower than attack at C_1. Transition structures **18** and **19** are both very high in energy due to the steric hindrance of the methyl group and the alkene. The product generated from transition state **19** was not located, since this specific conformation is very high in energy.
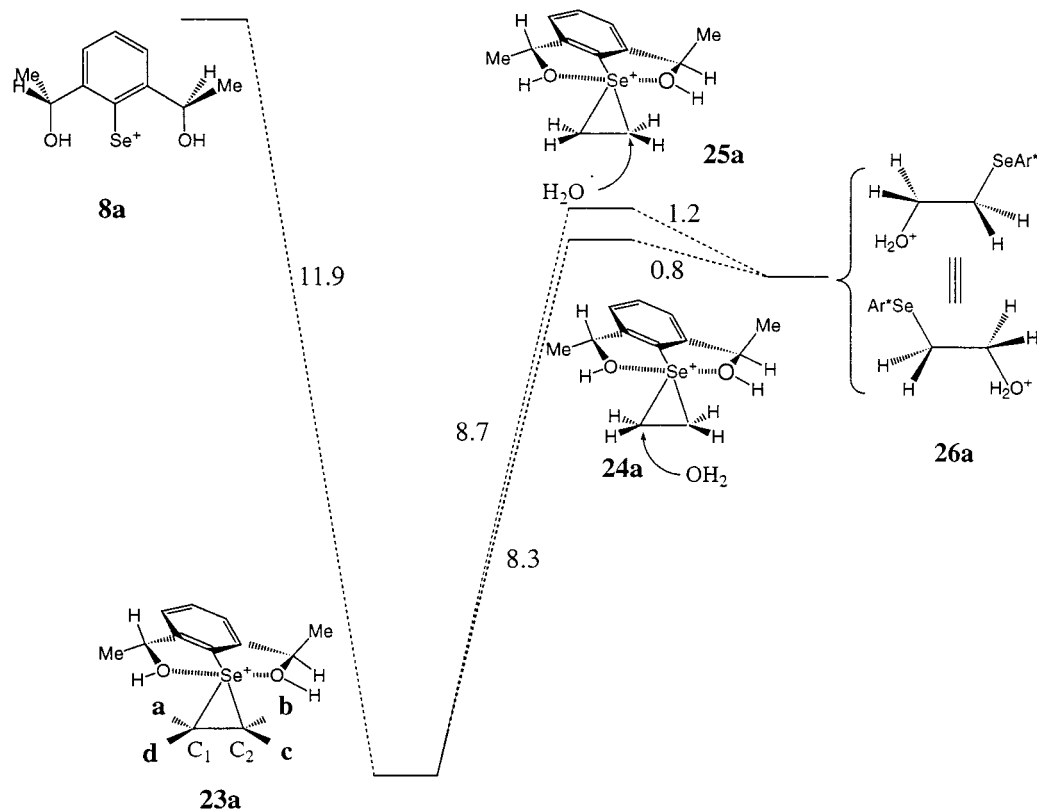
Stereoselectivities in Alkoxyselenenylations

J. Am. Chem. Soc., Vol. 121, No. 37, 1999 8571

Figure 7. Computed energetics for the reactions of a hydroxy model of the Déziel reagent with ethylene.
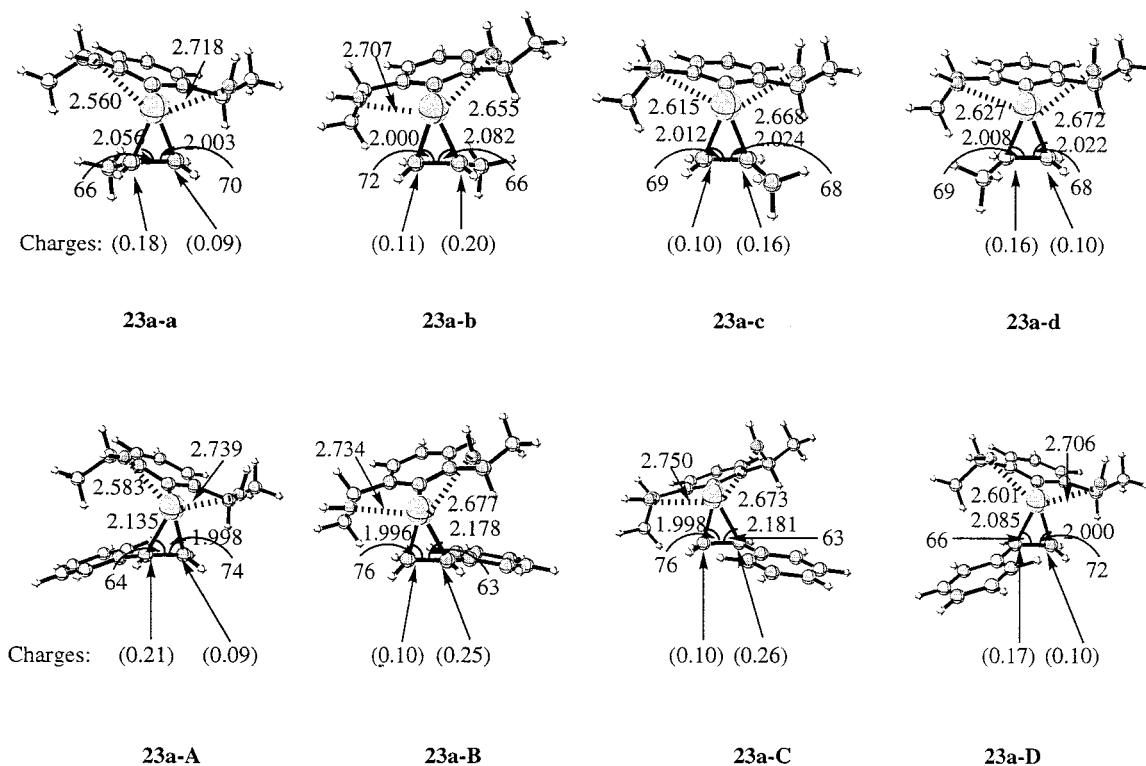

Figure 8. Geometrical parameters of the methyl- or phenyl-substituted intermediates of **23a** (distances in Å, angles in deg, numbers in parentheses are the sum of Mulliken charges of the carbon plus attached hydrogen and substitutents).

We also explored other models for Se coordination. The intermediate coordinated to HF instead of H_2O was optimized. Structure **20**, shown in Figure 6, has relatively short $Se-C_1$ and $Se-C_2$ bond lengths, 2.027 and 2.056 Å, respectively, similar to the water complex (**14**). In both, the bond length of $Se-C_2$ is longer than that of $Se-C_1$, suggesting that $Se-C_2$ can be more easily broken. The charge of C_2 is slightly more positive than that of C_1, which would direct the preference for nucleophilic attack as well.
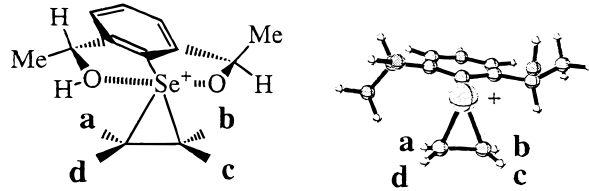
The intermediate becomes quite unsymmetrical upon substitution. Upon methyl substitution at position **b** (Figure 6, **21b**), the $Se-C_2$ bond is about 0.106 Å longer than the $Se-C_1$ bond.
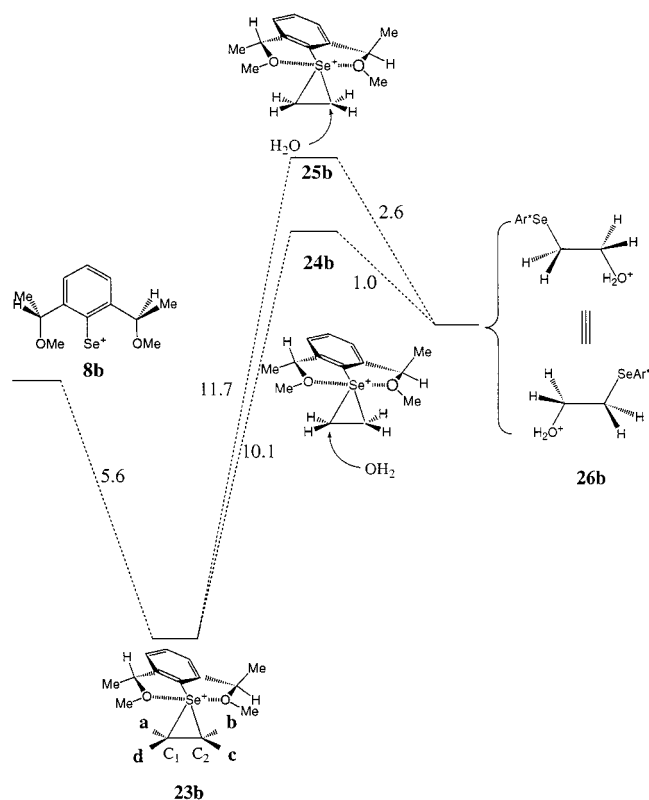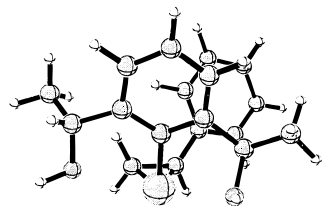
Figure 9. Computed energetics for the reaction of the Déziel reagent with ethylene.

Table 3. The Intermediate Formed from the Déziel Reagent and Ethylene with the Relative Energies of the Intermediates Substituted by Methyl or Phenyl, along with π-Stacking of Intermediate **23a-B** Shown below


substituent	a	b	c	d
methyl	2.3	1.4	0	0
tert-butyl	9.9	7.3	0	0.6
phenyl	1.3	0	0.3	0.4

23a-B

The charge on C_2 is 0.07 more positive than that of C_1. Phenyl has stronger influence on both the bond length and the charge distributions of C_1 and C_2 (Figure 6, **22b**). Phenyl substitution at position **b** causes the Se$-$C$_2$ bond to become 0.375 Å longer than Se$-$C$_1$, and the charge of C_2 is 0.30 more positive than that of C_1. These geometrical trends are observed for substitution at any of the four positions, as shown in Figure 6.

b. Model of the Déziel Reagent. The reactions of **8a** as a model for the selenium cation **3** were computed. The results
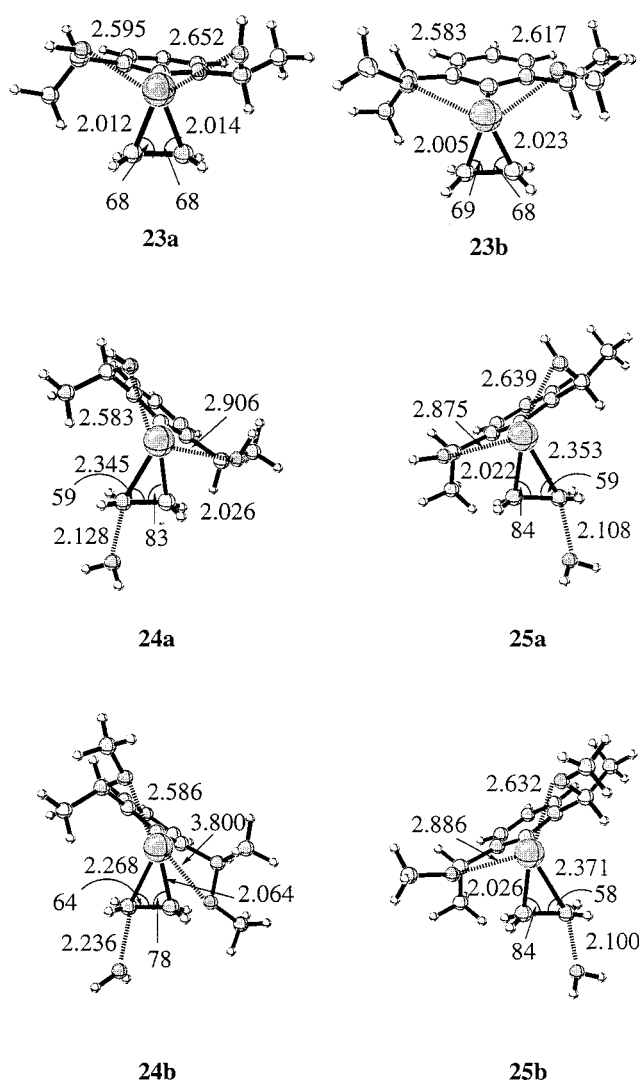

Figure 10. Geometrical parameters of the intermediates, **23a** and **23b**, and the transition states **24a**, **24b**, **25a**, and **25b** (distances in Å, angles in deg).
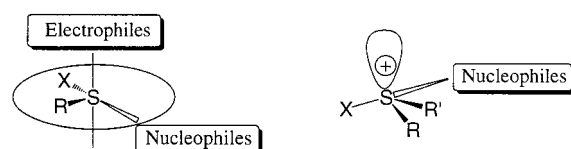
Figure 11. Arrangements of nonbonded ligands around the sulfur atom in crystal structures of divalent sulfides and trivalent sulfonium ions.

are shown in Figure 7. A water was not included in modeling selenium cation **3** because the selenium cation **3** has two oxygenated groups to coordinate the selenium. A water ligand should have no strong influence on the stereoselectivity. The alkene adds face to face with **8a**, similar to the addition of the alkene and **13**.[17] The relative energies of intermediates substituted by phenyl or methyl at each of the four positions are shown in Table 3. Phenyl substituents are most stable at position **b** (Table 3, **23a-B**), but **c** and **d** phenyls are only slightly less stable. Methyl substituents are equally stable at positions **c** and **d**, while the more sterically demanding *tert*-butyl group prefers **c**. More details of geometries of substituted intermediate **23a** are revealed in Figure 8.

(17) Oakley, R. T.; Reed, R. W.; Cordes, A. W.; Craig, S. L.; Graham, J. B. *J. Am. Chem. Soc.* **1987**, *109*, 7745−7749.
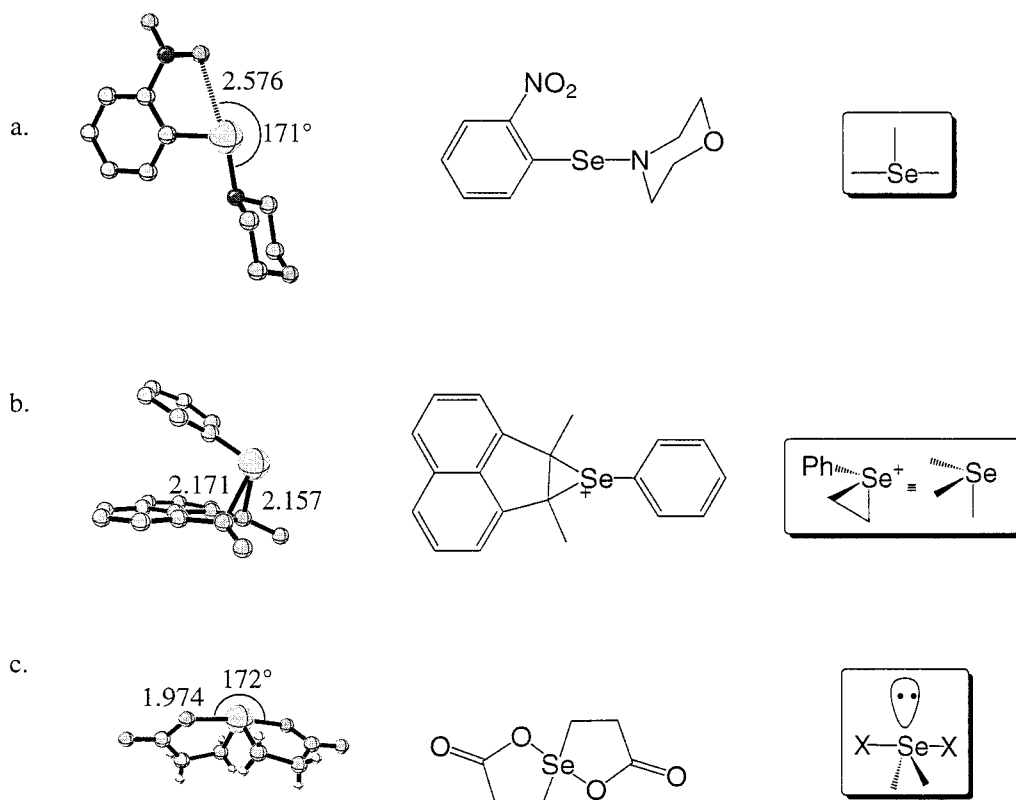
Figure 12. Geometries, structures, and ligand types of some di-, tri-, and tetravalent selenium compounds (distances in Å, and angles in deg).

The stereoselectivity is determined by nucleophilic attack on asymmetric intermediate, **23**. Figure 7 shows the various modes of attack on **23a**. Transition state **24a** is 0.4 kcal/mol lower energy than transition state **25a**. We also carried out calculations on the methoxy-substituted reagent that Déziel studied (Figure 9).

Transition state **24b** is 1.6 kcal/mol in lower energy than transition state **25b**. Attack as in **24a** and **24b** causes an H to move toward alkene; attack modes **25a** and **25b** causes methyl−alkene interaction. The former is favored. These transition states are shown in more detail in Figure 10.

3. Comparisons to Crystal Structures of Stable Selenium Compounds. Each of these structures exhibits four or five bonds. We thought it of interest to compare these with stable structures known from X-ray crystallography. It is well-known that nonbonded sulfur−oxygen contacts can influence the preferred geometries of sulfur−oxygen compounds, and similar interactions control geometries of Se−O compounds. As shown in Figure 11, electrophiles approach the sulfur atom from the 3p lone pair direction, the axial direction, while nucleophiles lie opposite to an X−S bond of sulfides or sulfonium compounds, the equatorial direction.[18] A few nucleophiles, atypically, are engaged in contacts perpendicular to the R−S−X plane. In most cases, the sulfur atom involved is part of a cation, or is covalently bonded to two electron-withdrawing atoms (nitrogens or oxygens).[19]

Selenium also prefers a trigonal bipyramidal geometry in hypervalent bonding. Investigations of more than 40 published crystal structures of organic, inorganic, and organometallic compounds containing multivalent selenides reveal that internal or external nucleophiles, such as the oxygens of nitro, carboxylate, hydroxy, or methoxy groups approach selenium along the extension of one of the bonds to selenium. For example, morpholino(*o*-nitrophenyl)selenide (Figure 12a) has planar geometry, where the oxygen of the nitro group contacts selenium with a distance of 2.576 Å, and the angle of oxygen−selenium−carbon of cyclohexyl is 171°.[20] The geometry of morpholino-(*o*-nitrophenyl)selenide is similar to the B3LYP/3-21G optimized geometries of **8** and **13**.

In tricoordinated seleniranium ions, the third bond is attached perpendicular to the selenide plane. One example is the seleniranium species formed by phenyl selenide with 1,2-dimethyl acenaphthylene (Figure 12b).[21] The selenium−carbon bonds of the seleniranium are 2.157 and 2.171 Å, respectively, with phenyl group on selenium π-stacking with the naphthalene ring, much as predicted for the preferred intermediates in the asymmetric alkoxyselenenylations.[22]

The geometries of tetravalent selenium compounds are trigonal bipyramidal with the lone pair electrons in one equatorial position and the electronegative oxygens apical. Nucleophiles or electron donors, such as the hydroxy group or carboxylate anion, contact selenium from apical positions, as shown in the crystalline geometry of a 1,6-dioxa-5-selenaspiro-(4.4)nonane-2,7-dione (Figure 12c).[23]

Nucleophilic ligands can interact with the LUMO of a Se−X bond to form a four-electron three-center bond. If selenium has a positive charge, the interactions between selenium and the ligand are stronger and the selenium−ligand distance is shorter.

(18) Bernardi, F.; Csizmadia, I. G.; Mangini, A. *Studies in Organic Chemistry 19, Organic Sulfur Chemistry: Theoreticaal and Experimental Advances;* Elsevier Science Publishers: New York, 1985; pp 218−219.

(19) Rosenfield, R. E., Jr.; Parthasarathy, R.; Dunitz, J. D. *J. Am. Chem. Soc.* **1977**, *99*, 4860−4862.

(20) Gicquel-Mayer, C.; Perez, G.; Lerouge, P.; Paulmier, C. *Acta Crystallogr., Sect. C (Cr. Str. Comm.)* **1987**, *43*, 284.

(21) Borodkin, G. I.; Gatilov, Y. V.; Rybalova, T. V.; Chernyak, E. I.; Shubin, V. G. *Izv. Akad. Nauk SSSR, Ser. Khim.* **1986**, 2832.

(22) Optimization of this structure with the B3LYP/3-21G method gives Se−C bond lengths as 2.1564 and 2.1571 Å, respectively.
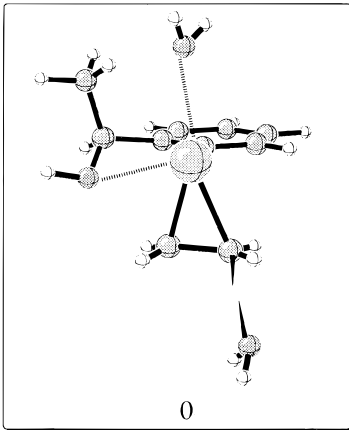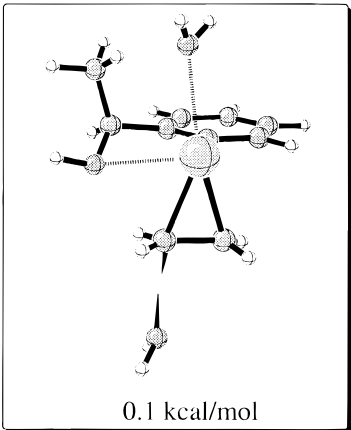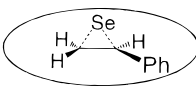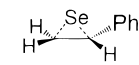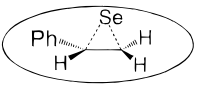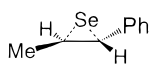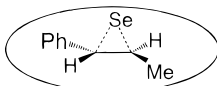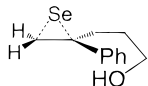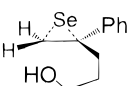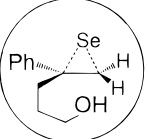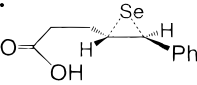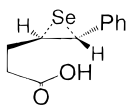
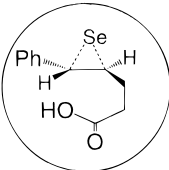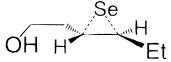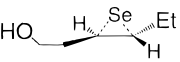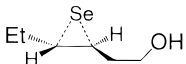(23) Dahlen, B.; Lindgren, B. *Acta Chem. Scand., Ser. A* **1979**, *33*, 403.

Table 4. The Favored Transition States of the Reactions of the Wirth Reagent with Ethylene along with the Possible Transition States Represented by Alkenes[a]

	0	0.1 kcal/mol

1.   83% d.e.

2.   72% d.e.

3.   78% d.e.

4.   72% d.e.

5.   0% d.e.

[a] The circled structures give the most stable transition states. These normally lead to the major products.

4. Selectivity Models. Calculations on the three model systems point to several factors controlling the stereoselectivities of alkoxyselenenylation. (1) Phenyl substituents on selenium prefer π-stacking with an alkene PhCH terminus (Table 2, **22a** and Table 3, **23a-B**); a phenyl in position **a** of **14** or position **b** of **23** is somewhat preferred over the unhindered positions **c** and **d**. (2) Bulky substituents such as methyl groups prefer positions **c** or **d** to minimize steric hindrance. (3) The alkene carbons, C_1 and C_2 are slightly different in the seleniranium intermediates; C_2 is the preferred site of nucleophilic attack in the case of **14** with transition state **17**, while C_1 is preferred in the case of **23** with transition state **24**, but the energy difference is quite small. (4) Phenyl groups stabilize positive charge better than alkyl and direct nucleophilic attack to the attached carbon. (5) Steric effects influence the direction of nucleophilic approach.

On the basis of these generalizations, Tables 4 and 5 summarize how the regio- and stereoselectivities of the asymmetric alkoxyselenenylations can be explained.

At the top of Table 4, the two low-energy transition states for attack of a nucleophile on the Wirth seleniranium ion are shown. The structure on the left will have the best cation-stabilizing group on the right-hand carbon, the site of attack of a nucleophile (here water). The transition structure shown at the right will have the cation-stabilizing substituent on the left-hand carbon. The drawings of the seleniranium intermediate shown in each row represent schematically the possible transition states.

For example, the left-hand structure in Table 4-1 will favor the transition state with phenyl in front, the sterically least-hindered position. This is the observed stereochemistry, and it is marked by the ellipse around the favored structure. For the right-hand transition state, the phenyl should go in back, because of the favorable π-stacking of the phenyls. This also corresponds to the experimental result. The two circled transition states will be the competing major transition states.

For the reaction of *trans-β*-methyl styrene (Tables 4-2), the phenyl will control the site of nucleophile attack. Consequently,

Table 5. Two Transition States of the Reaction of the Déziel Reagent with Ethylene along with the Possible Transition States Represented by Alkenes[a]

1				78% d.e.
2				55% d.e.
3				94% d.e.
4				86% d.e.
5				93% d.e.
6				80% d.e.
7				50% d.e.
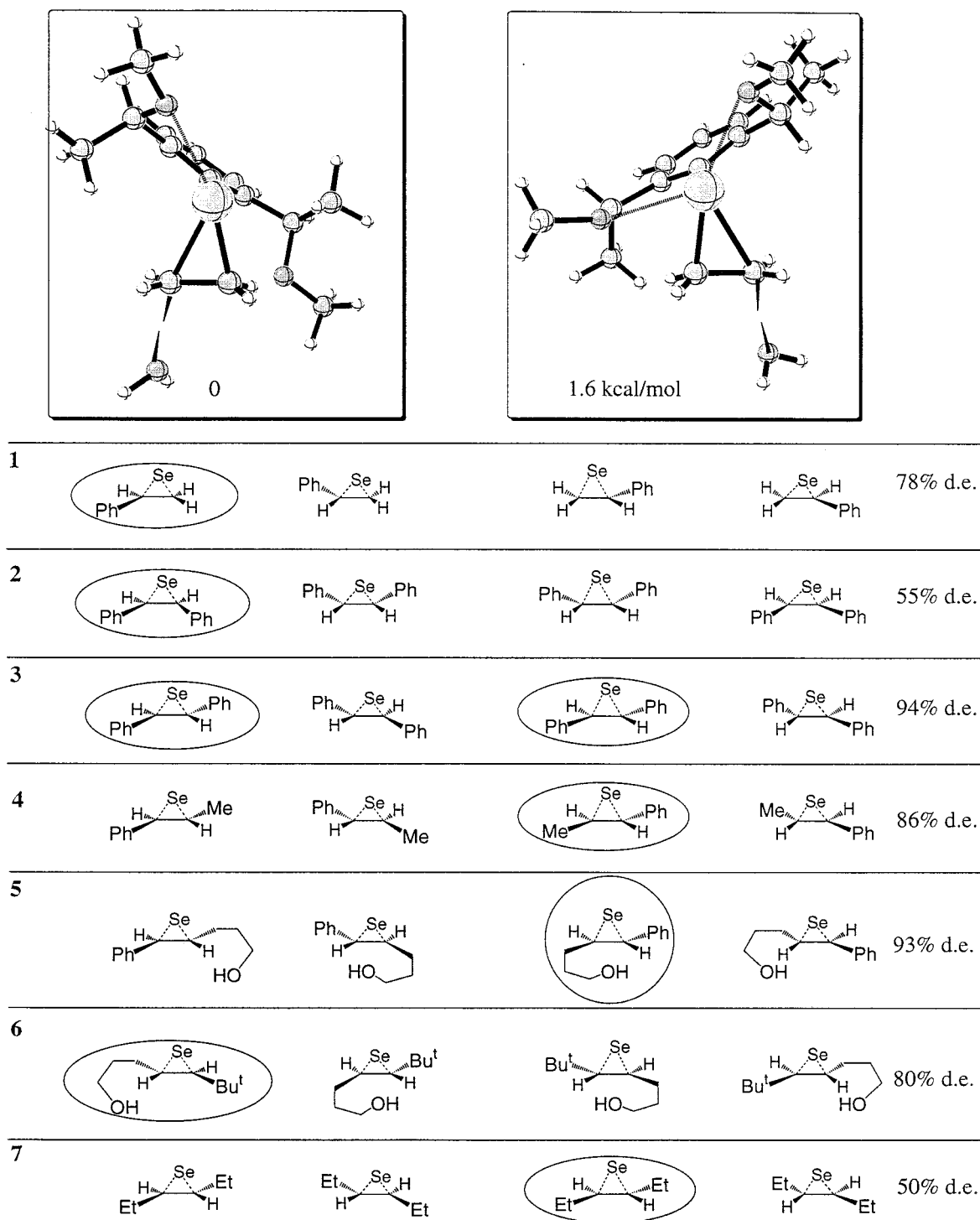
[a] The circled structures give the most stable transition states. These normally lead to the major products.

the four arrangements shown in Tables 4-2 are possible. The preferred transition state is circled, with the phenyl π-stacked and the methyl in the least-hindered arrangement. Entries 3−5 in Table 4 are examples of intramolecular trapping of the intermediate seleniranium intermediate. Entries 3 and 4 form transition states which place phenyl in the favored π-stacked arrangement, and alkyl in the front, where it is sterically unhindered. The last case (Tables 4 and 5) is one where there is no stereoselectivity, due to the fact that any transition state places one alkyl group in a disfavored arrangement.

Using a similar model, selectivities of reactions involve the Déziel reagent, **3**, can also be explained. The model of Déziel reagent has the opposite absolute configuration to the Wirth reagent; consequently, the most stable transition state **24** of nucleophilic attack is opposite to that of the Wirth reagent, **17**. In the drawing at the top of Table 5, the left-hand structure will be best when the cation-stabilizing group is at the site of attack, the left-hand carbon. The transition structure shown at the right will have the cation-stabilizing substituent on the right-hand carbon. The four possible transition states for substituted
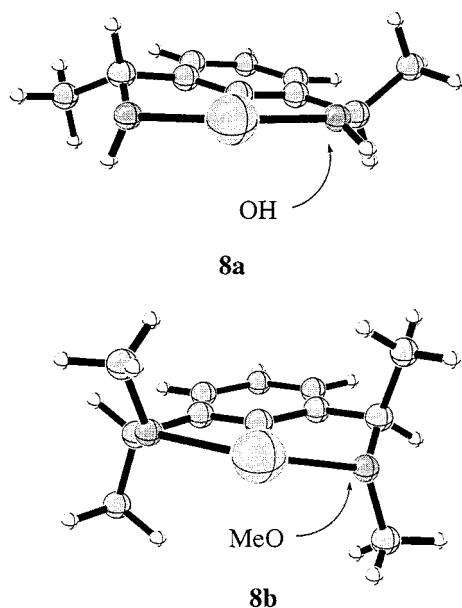
Figure 13. B3LYP/3-21G optimized geometries of the cation moieties of the Déziel reagent **3**.

Table 6. The Comparison of de of the Products from Reactions of Two Déziel's Selenium Reagents 27 (isomers of 3) and 28 with Alkenes

	27	28
Ph⌒ (styrene)	77.8	93.5
Ph⌒⌒COOH	85.7	>98.0
t-Bu⌒⌒⌒OH	80.0	87.5

alkenes are shown schematically in Table 5. In Tables 5-1, the left-hand structure will favor the transition state with phenyl group in front, and the right-hand transition state will favor the transition state with phenyl group at the back due to the π-stacking. Because the left-hand transition state is 1.6 kcal more stable than the right-hand transition state, the circled structure should dominate. This corresponds to the experimental result. In Tables 5-2, both structures will favor the transition states with phenyl groups in front. Since the transition state on the left side has lower energy, the structure in the circle should give the major product. This also fits the experimental result. For the reaction of *trans*-stilbene (Tables 5-3), the transition state circled with one phenyl π-stacked and the other unhindered, **b**, will be favored. This implies that the two transition states represented by the circled alkenes will be competing major transition states. In **4** and **5**, substituents, phenyl and methyl groups, control the stereoselectivity. Because phenyl prefers position **b** and methyl prefers position c or d, the structures in circles give the major product, which corresponds to products favored in the experiments.

Alkenes with *tert*-butyl substituents give *anti*-Markownikoff products due to steric factors.[24] When one substituent is a bulky *tert*-butyl group (Tables 5 and 6), the transition states with *tert*-butyl group at position **c** or **d** are favored. Position **c** is slightly favored, because the left-hand transition state has the lower energy. Alkenes *trans*-disubstituted with the same alkyl groups show low selectivities. In Tables 5−7, *trans*-3-pentene gives only 50% diastereoselectivity.

Calculations on transition states with the methoxy group used in the Déziel system show a larger difference (1.6 kcal/mol) than with hydroxyl groups (0.4 kcal). This is because the methyl group is bulkier than a hydrogen and the differences among the four positions on the two carbons of alkenes are enhanced (Figure 13). If the alkoxy groups on selenium reagents are bulkier, higher selectivities may be observed. In the experiments by Déziel et al., the selenium reagent **28** gives much higher de than **27** (Table 6).[25] Bulkier substituents such as *tert*-butyl groups instead of methyl groups may result in better chiral reagents.

(24) Patai, S. *The Chemistry of Double-Bonded Functional Groups, Part 2*; John Wiley & Sons: New York, 1989; pp 855−866.
(25) Déziel, R.; Malenfant, E.; Thibault, C.; Fréchette, S.; Gravel, M. *Tetrahedron Lett.* **1997**, *38*, 4753−4756.